European Radiology (2021) 31:1359–1366
https://doi.org/10.1007/s00330-020-07228-3

MAGNETIC RESONANCE

Hepatobiliary phase enhancement of liver metastases on gadoxetic acid MRI: assessment of frequency and patterns

Rajesh Bhayana[1] · Vinit Baliyan[1] · Hamed Kordbacheh[1] · Avinash Kambadakone[1]

Received: 28 May 2020 / Revised: 13 July 2020 / Accepted: 26 August 2020 / Published online: 4 September 2020

Abstract

Objectives To assess for and characterize patterns of hepatobiliary phase (HBP) enhancement in hepatic metastases of various malignancies on gadoxetic acid–enhanced MRI.

Methods Eighty gadoxetic acid–enhanced MRI studies performed between July 2012 and November 2019 in patients with hepatic metastases from 13 different primary malignancies were assessed. Most ($n = 60$) were from colorectal cancer (CRC), pancreatic ductal adenocarcinoma (PDAC), or neuroendocrine tumor (NET) primaries. Two radiologists quantitatively evaluated the dominant lesion on each MRI. A lesion was considered enhancing when HBP enhancement relative to muscle exceeded 20%. Lesions were classified by pattern of enhancement. Quantitative enhancement metrics and patterns of enhancement were compared between CRC, PDAC, and NET using non-parametric statistical tests.

Results Most dominant metastatic lesions > 1 cm (77%, 54/70) demonstrated HBP enhancement. HBP enhancement was identified in hepatic metastases from 10 different primary malignancies, including CRC, PDAC, and NET. PDAC metastases demonstrated a lower degree of HBP enhancement (26%) than CRC (44%, $p_{adj} = 0.04$) and NET (51%, $p_{adj} = 0.01$) metastases. Three discrete enhancement patterns were identified: peripheral, central (target), and diffuse heterogeneous. Patterns of HBP enhancement varied between CRC, PDAC, and NET, with secondary analysis demonstrating that PDAC had the highest proportion of peripheral pattern (73%, $p_{adj} < 0.001$), CRC the highest proportion of diffuse heterogeneous pattern (32%, $p_{adj} < 0.01$), and NET the highest proportion of central pattern (89%, $p_{adj} < 0.001$).

Conclusion Liver metastases from several primary malignancies, including PDAC, demonstrate mild HBP enhancement in variable patterns. Correlation with OATP1B3 expression and prognosis is required.

Key Points

- *Hepatobiliary phase (HBP) enhancement was identified in 77% of hepatic metastases in several different primary malignancies.*
- *Discrete patterns of HBP enhancement exist (peripheral, central, diffuse heterogeneous) and varied between CRC, PDAC, and NET. CRC and PDAC metastases demonstrated mostly non-central patterns (diffuse and peripheral), and NET mostly a central pattern.*
- *Relationship between HBP enhancement, enhancement pattern, OATP1B3 expression, and prognosis requires further dedicated exploration for each malignancy.*

Keywords Gadolinium ethoxybenzyl DTPA · Magnetic resonance imaging · Image enhancement · Liver neoplasms

✉ Rajesh Bhayana
rajesh.bhayana@uhn.ca

[1] Division of Abdominal Imaging, Department of Radiology, Massachusetts General Hospital, 55 Fruit St, White 270, Boston, MA 02114, USA

Abbreviations

CRC	Colorectal cancer
FOV	Field of view
GIST	Gastrointestinal stromal tumor
HBP	Hepatobiliary phase
HBP RER	Hepatobiliary phase relative enhancement ratio

HBP RIR	Hepatobiliary phase relative intensity ratio
NET	Neuroendocrine tumor
NEX	Number of excitations
NSCLC	Non–small cell lung cancer
OATP1B3	Organic anion transporter protein 1B3
PDAC	Pancreatic ductal adenocarcinoma
RCC	Renal cell carcinoma
ROI	Region of interest
TE	Echo time
TR	Repetition time

Introduction

Gadoxetic acid (Eovist/Primovist [Bayer HealthCare])–enhanced MRI is highly sensitive and specific in detecting colorectal cancer (CRC) liver metastases [1–5] and is the preferred imaging examination to identify CRC metastases, determine surgical eligibility, and facilitate operative planning [3, 4]. Favorable diagnostic performance has also been demonstrated for liver metastases from other primary malignancies, including pancreatic adenocarcinoma (PDAC) and neuroendocrine tumors (NET) [1, 6–8].

Gadoxetic acid is a "hepatocyte-specific" MRI contrast agent that is eliminated via the urinary and biliary systems in approximately equal parts. As a result, gadoxetic acid has properties similar to other extracellular contrast agents, followed by active intracellular hepatocyte uptake and biliary excretion that peaks about 20 min after injection [9]. Gadoxetic acid is transported into liver cells mostly due to expression of organic anion transporter protein 1B3 (OATP1B3) [1, 10]. The high sensitivity for metastases on hepatobiliary phase (HBP) imaging is attributed to the contrast between the hyperintense background liver and hypointense non-hepatocyte-containing metastases. Metastases have classically been described as non-enhancing on HBP [1, 10].

Some reports in the radiologic literature have recognized "paradoxical" or "atypical" HBP enhancement in hepatic metastases from breast and colorectal primaries [11, 12]. These studies have mostly described a "target" appearance on HBP images, with central enhancement attributed to contrast accumulation within fibrotic and necrotic tissue. A target pattern is also seen in fibrotic hepatic neoplasms such as intrahepatic cholangiocarcinoma, as fibrotic tissues accumulate extracellular contrast [13, 14]. However, HBP enhancement is also associated with OATP1B3 expression in CRC metastases, indicating that HBP enhancement in non-hepatocyte-containing lesions is not solely attributed to fibrosis [15].

A number of malignancies, including CRC and PDAC, demonstrate OATP1B3 expression [16, 17]. Since OATP1B3 expression has prognostic significance in some malignancies, HBP enhancement might serve as a useful biomarker [18]. Although PDAC expresses OATP1B3 and is commonly imaged with gadoxetic acid, there is an absence of literature documenting corresponding HBP enhancement. Various patterns of HBP enhancement have been sporadically reported in the literature, including "target" and "mixed hypointense," but require further exploration [11, 13, 14, 19]. The purpose of this study is to assess for and characterize hepatobiliary phase enhancement in hepatic metastases on gadoxetic acid–enhanced MRI.

Materials and methods

Patient cohort and study design

This was a retrospective study performed at a large quaternary care academic institution, with Institutional Review Board (IRB) approval and requirement for informed consent waived by the IRB. All data were collected and analyzed in compliance with the Health Insurance Portability and Accountability Act (HIPAA). All aspects of the study were performed in accordance with the Declaration of Helsinki.

Studies were retrieved from a search of our Picture Archiving and Communications System (PACS) for gadoxetic acid–enhanced MRI examinations performed between July 2012 and November 2019. Suitable studies were considered those with liver metastases. Exclusion criteria included as follows: lack of pathologic confirmation of hepatic metastases, isolated peripheral lesions that might be peritoneal, variable flip angles on pre-contrast and HBP images, severe motion artifacts on key sequences, and heterogeneous HBP enhancement of background liver parenchyma. Based on these criteria, out of 119 consecutive studies reviewed, 39 studies were excluded: 12 without pathologic confirmation, 3 with only superficial metastatic deposits (possibly peritoneal), 8 with different flip angles on pre-contrast and HBP images, 14 with motion artifacts that precluded quantitative analysis, and 2 with heterogeneous background liver parenchyma due to hemosiderosis. The final cohort for data analysis included 80 MRI studies. Basic demographic and clinical data was collected from medical records, including age, sex, and the temporal relationship of the MRI to systemic therapy (pre- or post-chemotherapy).

Imaging technique

All patients underwent gadoxetic acid–enhanced MRI of the abdomen on a 1.5- or 3-T MRI scanner at our institution with a phased array multi-channel body coil. Dynamic imaging was performed with axial 3-dimensional spoiled gradient-echo acquisitions with fat saturation after injection of 0.1 ml/kg gadoxetic acid. The pulse sequence parameters varied slightly by MRI machine, but representative parameters for the most

common pre-contrast and dynamic post-contrast images are as follows: 1.5 T, liver acquisition with volume acquisition (LAVA), flip angle 15, TR 2.35/TE 1.05, 0.73 NEX, FOV 400 × 400 mm^2, matrix 160 × 160, slice thickness 5 mm with 2.5 mm spacing. Delayed axial LAVA acquisitions were performed at 8 min with the same parameters as pre-contrast images, and at 20 min with either identical parameters or minimally increased TR/TE +/− slightly larger matrix (representative parameters for most common 20-min HBP acquisition: 1.5 T, LAVA, flip angle 15, TR 3.11/TE 1.44, 0.73 NEX, FOV 400 × 400 mm^2, matrix 256 × 256, slice thickness 5 mm with 2.5 mm spacing. Most importantly, any additional 20-min acquisitions acquired with a higher flip angle (most commonly 25) were not used in quantitative assessment. To our knowledge, pre- and post-contrast images are not differentially scaled. Although not directly quantitatively assessed or measured, a routine abdominal MRI protocol was also performed on each patient that generally included as follows: coronal and axial SSFSE (single-shot fast spin echo), diffusion-weighted images, ADC, and axial T1 in and out of phase.

Image analysis

Images were retrospectively reviewed by two radiologists (R.B. and V.B.) to identify and measure hepatic metastases. Region-of-interest (ROI) measurements were placed on the dominant hepatic lesion (one dominant hepatic lesion per MRI), paraspinal musculature, and background liver on pre-contrast and HBP images. ROI on hepatic metastatic lesions were drawn to be greater than 25 mm^2 for all lesions, at the location of highest intensity within the lesion. ROI measurements were used to calculate lesion-to-muscle and lesion-to-background liver ratios on pre-contrast and 20-min HBP images. To determine if lesions were enhancing and account for slight differences in pulse sequence parameters on HBP images, we assessed HBP enhancement relative to muscle (increase in lesion-to-muscle ratio), modified from a ratio used by Haimerl et al to quantify hepatic gadoxetic acid uptake [20]. HBP enhancement relative to muscle was calculated as follows:

$$\text{HBP enhancement relative to muscle (\%)} = \frac{\text{20-min lesion : muscle} - \text{Pre-contrast lesion : muscle}}{\text{Pre-contrast lesion : muscle}}$$

HBP enhancement relative to muscle > 20% was considered true enhancement. Although no threshold is defined in the literature regarding gadoxetic acid uptake, a 20% increase in ROI measurement to define enhancement was validated in renal lesions where pseudoenhancement did not exceed 13% (in pathologically proven cysts) and true enhancement exceeded 23% (in pathologically proven renal cell carcinomas) [21]. Previous studies assessing gadoxetic acid enhancement in metastatic lesions have used the lesion-to-background liver ratio on HBP (hepatobiliary phase relative intensity ratio [HBP RIR]) or increase in lesion-to-background liver ratio from pre-contrast to HBP images (hepatobiliary phase relative enhancement ratio [HBP RER]). We also calculated HBP RIR and HBP RER for dominant metastatic lesions.

Metastases were qualitatively subcategorized by pattern: peripheral, central (target), and diffuse heterogeneous. Lesions measuring < 1 cm were not subcategorized. On each MRI scan, the number of lesions demonstrating each pattern of uptake was counted, up to 10 for each pattern and 5 for subcentimeter lesions. The size of the largest lesion within each pattern was recorded.

Statistical analysis

Metastatic lesions were grouped by primary malignancy (CRC, $n = 30$; PDAC, $n = 20$; NET, $n = 10$; other, $n = 20$). For the three most common malignancies (CRC, PDAC, NET), characteristics were compared using non-parametric statistical tests. The Kruskal-Wallis test was used to compare quantitative measures of enhancement, number of lesions per MRI, and size of dominant lesions between groups. If a result was statistically significant, multiple comparisons were performed using Dunn's test to compare the individual groups, and p values were adjusted with the Benjamin-Hochberg method (p_{adj}). Fisher's exact test of independence was used to compare the proportion of dominant metastatic lesions that demonstrated enhancement, and the proportion of metastatic lesions that demonstrated each pattern of gadoxetic acid uptake (peripheral, central, diffuse) between groups. When significant results were obtained, pairwise comparisons were performed, and adjusted p values (p_{adj}) computed. Lesions with peripheral, central, and diffuse heterogeneous enhancement patterns were compared with respect to size, number of lesions, and HBP enhancement using the Kruskal-Wallis test. p values of less than 0.05 were considered to indicate a significant difference. All statistical analyses were performed in R (version 3.6.3; R Foundation for Statistical Computing).

Results

Patient demographics and descriptive statistics are summarized in Table 1. Of 80 patients, 44 were male (55%) and 36 were female (45%), with an average age of 60 years (range 27–84 years). Primary malignancies included CRC ($n = 30$), PDAC ($n = 20$), and NET ($n = 10$). The remainder ($n = 20$) had one of a heterogeneous group of primary malignancies (gastric, $n = 5$; medullary thyroid, $n = 4$; renal cell (RCC), $n = 2$; non–small cell lung cancer (NSCLC), $n = 2$;

Table 1 Descriptive statistics, stratified by primary malignancy. Number of MRI scans, number of metastases, demographic data, and temporal relationship of imaging examination to systemic therapy are noted

		Primary malignancy				
		Colorectal	Pancreatic adenocarcinoma	Neuroendocrine	Other*	Total
Number of MRI		30	20	10	20	80
Total number of metastases		202	118	127	138	585
Age (range)		60 (42–84)	64 (50–83)	55 (46–76)	58 (27–75)	60 (27–84)
Sex	Female (%)	10 (33)	8 (40)	7 (70)	11 (55)	36 (45)
	Male (%)	20 (67)	12 (60)	3 (30)	9 (45)	44 (55)
Treatment	Pre-Tx (%)	12 (40)	4 (20)	0 (0)	2 (10)	18 (22)
	Post-Tx (%)	18 (60)	16 (80)	10 (100)	18 (90)	62 (78)

*Heterogeneous group of malignancies (gastric, $n = 5$; thyroid, $n = 4$; renal cell, $n = 2$; non–small cell lung cancer, $n = 2$; esophageal, $n = 2$; transitional cell, melanoma, chordoma, gastrointestinal stromal tumor, and soft tissue sarcoma, $n = 1$ each)

esophageal, $n = 2$; transitional cell, melanoma, chordoma, gastrointestinal stromal tumor (GIST), and leiomyosarcoma, $n = 1$ each). In total, 585 metastatic lesions were identified in these patients, including 202 CRC, 118 PDAC, 127 NET, and 138 other metastases.

Hepatobiliary phase enhancement

Most (77%) dominant lesions > 1 cm demonstrated true HBP enhancement, including most of CRC (74%), PDAC (73%), NET (100%), and other (72%) dominant metastases. In the "other" category, HBP enhancement was identified in dominant hepatic metastases from gastric ($n = 4/5$), esophageal ($n = 2/2$), medullary thyroid ($n = 3/4$), bladder ($n = 1/1$), RCC ($n = 1/1$), GIST ($n = 1/1$), and leiomyosarcoma ($n = 1/1$). No HBP enhancement was identified in cases of NSCLC ($n = 2$), melanoma ($n = 1$), or chordoma ($n = 1$).

For CRC, PDAC, and NET, quantitative measures of HBP enhancement, enhancement patterns, number of metastatic lesions per study, and size of dominant lesions are displayed in Table 2. Median HBP enhancement relative to muscle was lower for PDAC metastases (26%) compared with those for CRC (44%, $p_{adj} = 0.04$) and NET (51%, $p_{adj} = 0.01$) metastases. No statistically significant difference was detected between CRC and NET metastases (44 vs 51%, $p_{adj} = 0.26$). The distribution of HBP enhancement relative to muscle for metastases from each primary malignancy is displayed in Fig. 1.

Median hepatobiliary phase relative intensity ratios (HBP RIR) for enhancing (0.47) and non-enhancing (0.53) CRC metastases were not significantly different ($p = 0.96$). PDAC metastases demonstrated a higher HBP RIR for enhancing lesions (0.48) compared with non-enhancing lesions (0.35) ($p = 0.02$). For both CRC and PDAC, hepatobiliary phase relative enhancement ratio (HBP RER) was significantly higher in enhancing lesions (75, 77%) than in non-enhancing lesions (66, 62%) ($p = 0.01$, 0.02).

Patterns of HBP enhancement

Patterns of enhancement observed, including peripheral, central/target, and diffuse heterogeneous patterns, are illustrated in Fig. 2. Primary analysis of dominant lesions demonstrated that proportions of each pattern of enhancement differed between CRC, PDAC, and NET ($p < 0.001$). In secondary analysis, PDAC metastases had a significantly higher proportion of the peripheral pattern (73%) than CRC (41%) and NET (8.9%) metastases ($p_{adj} < 0.001$ for both); NET metastases had a higher proportion of the central pattern (89%) compared with each of the other groups (CRC, 27%; PDAC, 18%; $p_{adj} < 0.001$ for both); and CRC metastases had a higher proportion of the diffuse heterogeneous pattern (32%) compared with PDAC (9.1%, $p_{adj} = 0.006$) and NET (2.5%, $p_{adj} < 0.001$) metastases, despite the peripheral pattern being the most common pattern identified in CRC metastases (41%).

Median dominant lesion size did not significantly differ between patterns of enhancement (peripheral = 28 mm; central = 18 mm; diffuse = 20 mm; $p = 0.10$). There was no difference in the median number of hepatic metastases per patient between patterns (7 peripheral; 8 central; 8 diffuse; $p = 0.40$). HBP enhancement relative to muscle was not equivalent between patterns of enhancement ($p = 0.04$). However, pairwise comparisons only demonstrated a tendency for the central pattern to enhance more than the diffuse (50 vs 26%, $p_{adj} = 0.06$) and peripheral patterns (50 vs 37%, $p_{adj} = 0.12$) that did not reach statistical significance.

Discussion

Hepatic metastases have classically been described as non-enhancing on hepatobiliary phase. But some studies have demonstrated HBP enhancement in metastases from breast and colon primaries, relating to fibrotic components in

Table 2 Characteristics of metastatic lesions, stratified by primary malignancy (colorectal cancer, pancreatic ductal adenocarcinoma, neuroendocrine tumor). Specifically, quantitative measures of enhancement in dominant lesions, pattern of enhancement for both dominant and all metastatic lesions, number of metastatic lesions per MRI, and size of dominant lesion are displayed for each group

		Primary Malignancy			
		Colorectal	Pancreatic adenocarcinoma	Neuroendocrine	*p* value*
Dominant lesion	Enhancing (%)	20 (74)	11 (73)	10 (100)	0.21
	Non-enhancing (%)	7 (26)	4 (27)	0 (0)	
	< 1 cm	3	5	*0*	
HBP[a] enhancement relative to muscle (median, enhancing lesions, %)		44	26	51	**0.01**
HBP RIR[b] (median)	+/–**	0.47/0.53	0.48/0.35	0.50/-	0.66/0.13
HBP RER[c] (median)	+/− (%)	75/66	77/62	81/-	0.54/0.71
Dominant pattern					**< 0.001**
	Peripheral (%)	7 (35)	8 (72.7)	0 (0)	**< 0.001**
	Central (%)	6 (30)	1 (9.1)	10 (100)	**< 0.001**
	Diffuse (%)	7 (35)	2 (18.2)	0 (0)	0.10
All metastases, pattern					**< 0.001**
Signal pattern (qualitative, > 1 cm)	Peripheral (%)	35 (41)	32 (73)	7 (8.9)	**< 0.001**
	Central (%)	23 (27)	8 (18)	70 (89)	**< 0.001**
	Diffuse (%)	27 (32)	4 (9.1)	2 (2.5)	**<0.001**
Subcentimeter		71	70	48	
Number of metastases per MRI (median [IQR[d]])		5.5 [2.3–9.8]	5.0 [3–7.3]	15 [8–15]	**0.004**
Size of dominant lesion (median [IQR[d]], mm)		25 [18–45]	20 [16–26]	19 [17–24]	0.36

*p value for comparison between all three groups is displayed, where appropriate. Where $p < 0.05$ (in bold), pairwise comparisons were performed to further assess. Results of the pairwise comparisons are described in the "Results" section

**+/− refers to enhancing (+) and non-enhancing (−) lesions

[a] *HBP* hepatobiliary phase

[b] *HBP RIR* hepatobiliary phase relative intensity ratio (lesion-to-liver ratio, 20-min HBP images)

[c] *HBP RER* hepatobiliary phase relative enhancement ratio (increase in lesion-to-liver ratio from pre-contrast to 20-min HBP images)

[d] *IQR* interquartile range

"target" lesions and correlating with OATP1B3 expression in CRC metastases [11, 12, 15]. OATP1B3 has potential prognostic significance, so HBP enhancement might serve as a biomarker in malignancies that express OATP1B3, including CRC and PDAC. But, to our knowledge, the presence of HBP enhancement has not been reported in most malignancies, including PDAC. We found HBP enhancement in hepatic metastases from 10 different primary malignancies, of which 77% of dominant lesions demonstrated HBP enhancement. For PDAC, 73% of dominant metastases demonstrated HBP enhancement, with levels of enhancement lower than CRC and NET metastases.

Patterns of HBP enhancement, illustrated in Fig. 2, varied by primary malignancy. PDAC and CRC metastases had the highest proportion of peripheral and diffuse HBP enhancement patterns, respectively, and NET metastatic lesions had the highest proportion of central (target) HBP enhancement. Both primary and secondary hepatic malignancies have a central (target) HBP enhancement pattern due to extracellular accumulation of contrast in areas of fibrosis [11, 13, 14, 19]. The pathologic correlate for non-central HBP enhancement in non-hepatocyte-containing lesions is less clear. Park et al demonstrated that HBP enhancement in "mixed hypointense" appearing CRC metastases correlated with OATP1B3 expression and had prognostic significance [15]. The predominance of non-central patterns of HBP enhancement in CRC and PDAC, both of which express OATP1B3, raises the possibility that non-central HBP enhancement might be due to OATP1B3 expression. However, this requires histologic correlation.

Despite differences in measurement technique, our finding that HBP enhancement is common in colorectal metastases is similar to those in other studies in the literature [12, 15, 19]. Most reports of HBP enhancement in metastatic lesions define

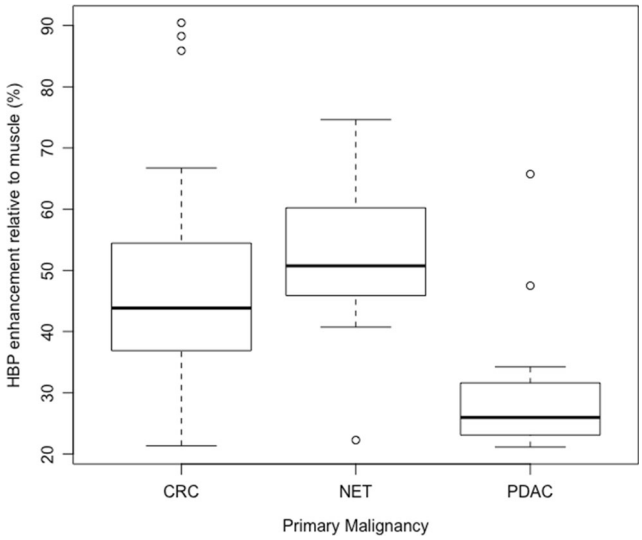

Fig. 1 Boxplot of hepatobiliary phase (HBP) enhancement relative to muscle for liver metastases by primary malignancy. PDAC metastases had lower levels of enhancement on HBP phase than CRC and NET

enhancement in relation to background liver parenchyma [11, 15, 19]. Since liver parenchyma demonstrates variable uptake on HBP images [20], we felt this technique would be less reliable in assessing for true HBP enhancement. Our finding of HBP enhancement in hepatic metastases from PDAC, NET, and several other malignancies, to our knowledge, has not been reported. Radiologists should be aware of this phenomenon in hepatic metastases from primary tumors other than CRC and breast cancer.

The relative intensity of lesion-to-liver ratio on HBP (HBP RIR) likely correlates with a radiologist's ability to perceive enhancement within a lesion, given that it measures contrast between the lesion and background liver. However, HBP RIR only correlated with true enhancement related to muscle in PDAC, and not in CRC. HBP RER (increase in HBP RIR from pre-contrast to HBP) correlated with true enhancement for both PDAC and CRC, suggesting that it is more reliable. Measurements of HBP RIR to assess for HBP enhancement should be avoided in future studies. Our findings suggest that our ability to perceive true enhancement on HBP images alone is limited, as we might expect given variable background liver uptake. All enhancing metastases in our series had a HBP RIR lower than 1, indicating they remained hypointense relative to background liver.

For CRC, studies have documented that HBP enhancement correlates with OATP1B3 expression, can help predict early treatment response [22], and is associated with improved overall survival [23]. Our novel finding of HBP enhancement

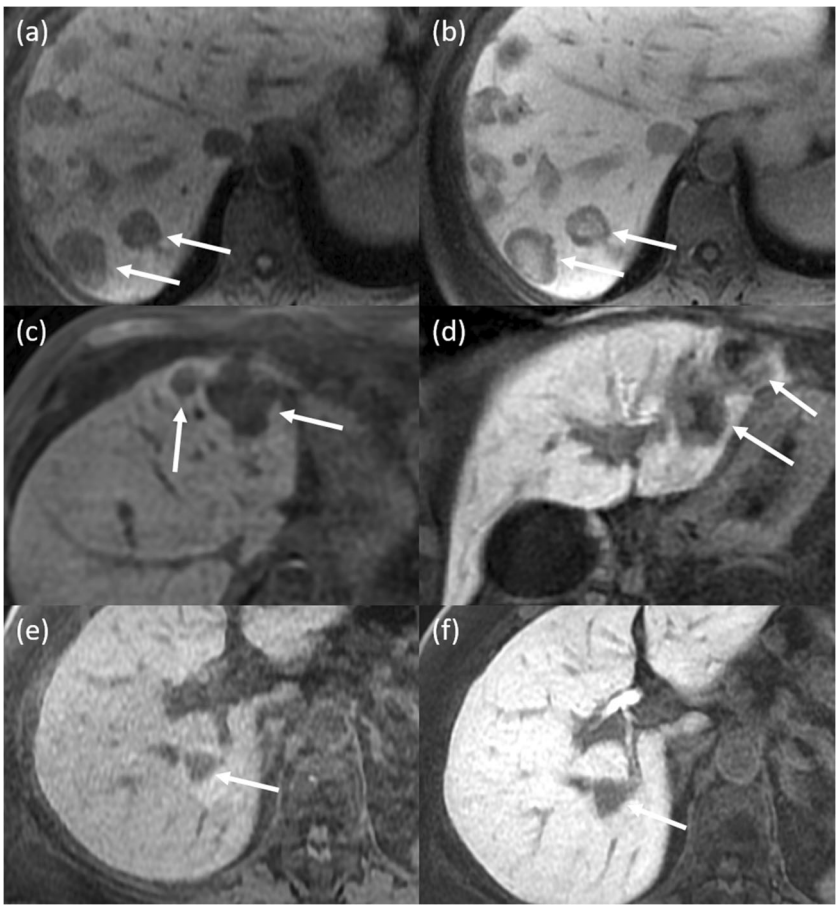

Fig. 2 Patterns of hepatobiliary phase (HBP) enhancement observed in metastases. Axial pre-gadolinium T1W image (**a**) and corresponding HBP image (**b**) in a 55-year-old man with neuroendocrine metastases demonstrate a central pattern of HBP enhancement (arrows). Axial pre-gadolinium T1W image (**c**) and coronal HBP image (**d**) in a 74-year-old man with pancreatic cancer demonstrate a peripheral pattern of HBP enhancement (arrows). Axial pre-gadolinium T1W image (**e**) and corresponding axial HBP image (**f**) in a 48-year-old woman with colorectal cancer demonstrate a diffuse pattern of enhancement. At quantitative assessment, the dominant lesion in all three of these patients demonstrated HBP enhancement

in hepatic metastases from several other primary malignancies needs to be further explored, especially in PDAC which is known to express OATP1B3. Organic anion transporting polypeptides (OATP) are a family of transport proteins that have a role in the influx of a number of substrates into cells, including various pharmacologic agents used for chemotherapeutic treatment [24]. Both OATP1B1 and 1B3, for example, have a role in cellular uptake of irinotecan-based chemotherapy commonly used in CRC and PDAC [25]. The expression of transporters such as OATP1B3 has potential for use as a biomarker, as a drug target, and for prognostication [17, 25, 26]. Dedicated exploration of HBP enhancement in hepatic metastases from malignancies other than CRC is required, specifically assessing its relationship with pathologic findings, OAT1B3 expression levels, and prognosis. In PDAC, OATP1B3 expression is higher in primary lesions of earlier stage, so quantification of gadoxetic acid uptake in primary pancreatic lesions is also of interest [27].

There are a few limitations to our study. Histopathologic and clinical correlation was unavailable, and HBP enhancement could not be correlated with OATP1B3 expression and specific pathologic findings. This was a retrospective study performed at a single institution, which limits its generalizability. Although primary analyses were performed on single dominant lesions only, secondary analyses included several lesions per patient, which introduced clustering bias.

In conclusion, HBP enhancement was common in hepatic metastases from several primary malignancies and was identified in several malignancies where HBP enhancement has not been previously reported. Discrete patterns of HBP enhancement included peripheral, central (target), and diffuse heterogeneous patterns. The central (target) pattern, seen in primary and secondary tumors due to extracellular accumulation of contrast in fibrotic tissues, was more common in NET than in CRC and PDAC metastases. Non-central patterns were more common in CRC and PDAC, which are both known to express OATP1B3. Future studies are required to elucidate the relationship between HBP enhancement, enhancement pattern, OATP1B3 expression, and prognosis for PDAC and other primary malignancies.

Funding The authors state that this work has not received any funding.

Compliance with ethical standards

Guarantor The scientific guarantor of this publication is Avinash Kambadakone.

Conflict of interest Avinash Kambadakone has received research grants from both GE Healthcare and Philips.

The other authors of this manuscript declare no relationships with any companies whose products or services may be related to the subject matter of the article.

Statistics and biometry No complex statistical methods were necessary for this paper.

Informed consent Written informed consent was waived by the Institutional Review Board.

Ethical approval Institutional Review Board approval was obtained.

Methodology
- Retrospective
- Observational
- Performed at one institution

References

1. Chen L, Zhang J, Zhang L et al (2012) Meta-analysis of gadoxetic acid disodium (Gd-EOB-DTPA)-enhanced magnetic resonance imaging for the detection of liver metastases. PLoS One 7:e48681
2. Hammerstingl R, Huppertz A, Breuer J et al (2008) Diagnostic efficacy of gadoxetic acid (Primovist)-enhanced MRI and spiral CT for a therapeutic strategy: comparison with intraoperative and histopathologic findings in focal liver lesions. Eur Radiol 18:457–467
3. Scharitzer M, Ba-Ssalamah A, Ringl H et al (2013) Preoperative evaluation of colorectal liver metastases: comparison between gadoxetic acid-enhanced 3.0-T MRI and contrast-enhanced MDCT with histopathological correlation. Eur Radiol 23:2187–2196
4. Zech CJ, Korpraphong P, Huppertz A et al (2014) Randomized multicentre trial of gadoxetic acid-enhanced MRI versus conventional MRI or CT in the staging of colorectal cancer liver metastases. Br J Surg 101:613–621
5. Jhaveri K, Cleary S, Audet P et al (2015) Consensus statements from a multidisciplinary expert panel on the utilization and application of a liver-specific MRI contrast agent (gadoxetic acid). AJR Am J Roentgenol 204:498–509
6. Motosugi U, Ichikawa T, Morisaka H et al (2011) Detection of pancreatic carcinoma and liver metastases with gadoxetic acid-enhanced MR imaging: comparison with contrast-enhanced multidetector row CT. Radiology 260:446–453
7. Tirumani SH, Jagannathan JP, Braschi-Amirfarzan M et al (2018) Value of hepatocellular phase imaging after intravenous gadoxetate disodium for assessing hepatic metastases from gastroenteropancreatic neuroendocrine tumors: comparison with other MRI pulse sequences and with extracellular agent. Abdom Radiol (NY) 43:2329–2339
8. Giesel FL, Kratochwil C, Mehndiratta A et al (2012) Comparison of neuroendocrine tumor detection and characterization using DOTATOC-PET in correlation with contrast enhanced CT and delayed contrast enhanced MRI. Eur J Radiol 81:2820–2825
9. Hamm B, Staks T, Mühler A et al (1995) Phase I clinical evaluation of Gd-EOB-DTPA as a hepatobiliary MR contrast agent: safety, pharmacokinetics, and MR imaging. Radiology 195:785–792
10. Reimer P, Rummeny EJ, Shamsi K et al (1996) Phase II clinical evaluation of Gd-EOB-DTPA: dose, safety aspects, and pulse sequence. Radiology 199:177–183
11. Ha S, Lee CH, Kim BH et al (2012) Paradoxical uptake of Gd-EOB-DTPA on the hepatobiliary phase in the evaluation of hepatic metastasis from breast cancer: is the "target sign" a common finding? Magn Reson Imaging 30:1083–1090
12. Granata V, Catalano O, Fusco R et al (2015) The target sign in colorectal liver metastases: an atypical Gd-EOB-DTPA "uptake"

on the hepatobiliary phase of MR imaging. Abdom Imaging 40: 2364–2371
13. Chong YS, Kim YK, Lee MW et al (2012) Differentiating mass-forming intrahepatic cholangiocarcinoma from atypical hepatocellular carcinoma using gadoxetic acid-enhanced MRI. Clin Radiol 67:766–773
14. Yoshikawa J, Matsui O, Kadoya M, Gabata T, Arai K, Takashima T (1992) Delayed enhancement of fibrotic areas in hepatic masses: CT-pathologic correlation. J Comput Assist Tomogr 16:206–211
15. Park SH, Kim H, Kim EK et al (2017) Aberrant expression of OATP1B3 in colorectal cancer liver metastases and its clinical implication on gadoxetic acid-enhanced MRI. Oncotarget 8:71012–71023
16. Pressler H, Sissung TM, Venzon D, Price DK, Figg WD (2011) Expression of OATP family members in hormone-related cancers: potential markers of progression. PLoS One 6:e20372
17. Obaidat A, Roth M, Hagenbuch B (2012) The expression and function of organic anion transporting polypeptides in normal tissues and in cancer. Annu Rev Pharmacol Toxicol 52:135–151
18. Lee W, Belkhiri A, Lockhart AC et al (2008) Overexpression of OATP1B3 confers apoptotic resistance in colon cancer. Cancer Res 68:10315–10323
19. Kim A, Lee CH, Kim BH et al (2012) Gadoxetic acid-enhanced 3.0T MRI for the evaluation of hepatic metastasis from colorectal cancer: metastasis is not always seen as a "defect" on the hepatobiliary phase. Eur J Radiol 81:3998–4004
20. Haimerl M, Verloh N, Zeman F et al (2017) Gd-EOB-DTPA-enhanced MRI for evaluation of liver function: comparison between signal-intensity-based indices and T1 relaxometry. Sci Rep 7:43347
21. Al Salmi IS, Halperin J, Al-Douri F, Leung V, Patlas M, Alabousi A (2019) Validation of region of interest measurements for the objective assessment of post-contrast enhancement of renal lesions on MRI. Br J Radiol 92:20190507
22. Murata S, Matsushima S, Sato Y et al (2018) Predicting chemotherapeutic response for colorectal liver metastases using relative tumor enhancement of gadoxetic acid disodium-enhanced magnetic resonance imaging. Abdom Radiol (NY) 43:3301–3306
23. Cheung HMC, Karanicolas PJ, Coburn N, Seth V, Law C, Milot L (2019) Delayed tumour enhancement on gadoxetate-enhanced MRI is associated with overall survival in patients with colorectal liver metastases. Eur Radiol 29:1032–1038
24. Schulte RR, Ho RH (2019) Organic anion transporting polypeptides: emerging roles in cancer pharmacology. Mol Pharmacol 95: 490–506
25. Teft WA, Welch S, Lenehan J et al (2015) OATP1B1 and tumour OATP1B3 modulate exposure, toxicity, and survival after irinotecan-based chemotherapy. Br J Cancer 112:857–865
26. Wright JL, Kwon EM, Ostrander EA et al (2011) Expression of SLCO transport genes in castration-resistant prostate cancer and impact of genetic variation in SLCO1B3 and SLCO2B1 on prostate cancer outcomes. Cancer Epidemiol Biomarkers Prev 20:619–627
27. Hays A, Apte U, Hagenbuch B (2013) Organic anion transporting polypeptides expressed in pancreatic cancer may serve as potential diagnostic markers and therapeutic targets for early stage adenocarcinomas. Pharm Res 30:2260–2269